



OPEN

Remineralization of early enamel lesions with a novel prepared tricalcium silicate paste

Kareem Hamdi¹, Hamdi H. Hamama^{2✉}, Amira Motawea³, Amr Fawzy⁴ & Salah Hasab Mahmoud²

To evaluate the remineralization potential of prepared tricalcium silicate (TCS) paste compared to silver diamine fluoride-potassium iodide (SDF-KI) and casein phosphopeptide-amorphous calcium phosphate (CPP-ACP) on artificial enamel lesions. Thirty permanent sound molars were collected for the study. After cleaning, root cutting, and applying acid-resistant nail varnish, leaving a 4 × 4 mm buccal window, the teeth were subjected to demineralization process. The teeth were divided into three treatment groups (n = 10). In each group, the teeth were sectioned buccolingually to obtain two halves (30 self-control and 30 experimental halves). The self-control halves were subjected to cross-sectional microhardness (CSMH), energy-dispersive X-ray spectroscopy at 50, 100, and 150 μm from the external enamel surface, and micromorphological analysis at the superficial enamel surface. The experimental halves were subjected to the same tests after 30 days of remineralization. Three-way analysis of variance (ANOVA) outcomes showed no significant difference in CSMH after treatment among the three different groups at the different levels (p > 0.05). Meanwhile, three-way ANOVA outcomes showed a significant difference in calcium/ phosphate ratio after treatment among the three different groups at the different levels. (p < 0.05). The tricalcium silicate paste used in this study showed potential remineralization in subsurface enamel lesions.

The first clinical sign of enamel demineralization is a white spot lesion (WSL). The demineralization process becomes confined within the superficial enamel layer leading to marked porosity. According to the International Caries Detection and Assessment System (ICDAS), WSLs can be categorized into scores 1 and 2. ICDAS score 1 is characterized by the appearance of WSLs after a relatively prolonged air surface drying. In ICDAS score 2, WSLs are obvious in dry and wet conditions¹. In both scores, the structural integrity of the enamel is maintained and intact with no localized breakdown. When these lesions are left untreated, they might progress to a continuous loss of minerals and break down until cavitation². Current cariology research focused on the effectiveness of the application of some remineralizing agents that maintained ion supersaturation in the oral environment surrounding these lesions. This might enhance calcium and phosphate ions to fill the formed microspores and stop further mineral loss³.

Fluoride has been considered the most popular remineralizing agent in the past decades. Fluoride can inhibit plaque biofilm and enhance calcium and phosphate ion precipitation within the biofilm⁴. Several laboratory studies have assumed that fluoride ions can replace the -OH group in the hydroxyapatite (HAp)-forming fluorapatite, which has superior resistance to acidic attacks⁵. The medical treatment of early enamel carious lesions encompassed the use of fluoride-based remineralizing agents, such as sodium fluoride and stannous fluoride⁶. Recently, silver diamine fluoride (SDF) has gained wide acceptance in the prevention and treatment of these early enamel lesions⁶. In 2014, the U.S. Food and Drug Administration approved SDF as caries arrest therapy for adults and children⁶. The caries arrest ability of SDF has shown marked superiority over other fluoride-based products, such as sodium fluoride and stannous fluoride^{7,8}. In addition to its superior role in caries prevention and arrest, several laboratory studies have also assessed its remineralization power^{9,10}.

Nowadays, non-fluoride (bioavailable calcium phosphate) remineralizing agents are considered the gold standard medical treatment for early enamel carious lesions. This category of bioactive remineralizing agents includes amorphous calcium phosphate (ACP), casein phosphopeptide (CPP-ACP), and tricalcium phosphate¹¹.

¹Operative Department, Faculty of Dentistry, Zagazig University, Zagazig, Egypt. ²Operative Dentistry Department, Faculty of Dentistry, Mansoura University, Algomhoria St, Mansoura City 35516, Egypt. ³Department of Pharmaceutics, Faculty of Pharmacy, Mansoura University, Mansoura, Egypt. ⁴UWA Dental School, University of Western Australia, Perth, Australia. ✉email: hamdy@connect.hku.hk

Material	Composition	Manufacture
Riva star	<ul style="list-style-type: none"> • Silver capsule: containing silver fluoride • Green capsule: containing KI 	SDI Ltd., Bayswater, VIC 3153 Australia
Tooth mousse	CPP-ACP	GC Europe N.V
TCS paste	<ul style="list-style-type: none"> • 5% (w/v) TCS • 2.5% (w/v) gelatin • 2.5% (w/v) carboxymethyl cellulose (CMC) • 2% (w/v) propylene glycol • 0.1% (w/v) methylparaben • Distilled water 	Prepared at the Department of Pharmaceutics, Faculty of Pharmacy, Mansoura University

Table 1. Materials used in the study.

CPP-ACP is phosphorylated casein extracted from milk. Its remineralization power is ascribed to the chemical effect of phosphorylated casein in addition to the presence of calcium and phosphate ions¹². At low pH, ACP separates from CPP, which usually increases the salivary saturation with Ca^{2+} and PO_4^{3-} ions. After this separation, CPP can stabilize ACP in the oral biofilm, providing an amorphous state of supersaturation to maintain alkaline pH and enhance the remineralization process^{13,14}.

Calcium silicate-based materials ($\beta\text{-CaSiO}_3$, $\beta\text{-Ca}_2\text{SiO}_4$, and Ca_3SiO_4) play an important role in hard tissue regeneration. It shows good bioactivity, biocompatibility, and the ability to induce bone-like appetite formation. Most literature about these materials highlights their reparative role in restorative and endodontic fields. Current scientific literature shows little evidence suggesting using these materials in the medical management of early enamel lesions. When tricalcium silicate (TCS; Ca_3SiO_4) comes into contact with saliva, it dissolves and deposits the silanol group (Si–O) on the enamel surface¹⁵. This functional group can bind to Ca^+ ions and induce HAP precipitation. Furthermore, the salivary phosphate group (PO_4^{3-}) can attract Ca^{2+} ions through the silanol group, forming a calcium phosphate (Ca–P)-rich layer that plays a great role in enamel remineralization¹⁵. Another in vitro study has emphasized the remineralization effect of combined TCS with fluoride on demineralized enamel¹⁶. TCS was used in the slurry form in the literature^{15,16}.

Considering the limited evidence suggesting the remineralization of early enamel lesions using TCS, this study was designed to evaluate the remineralization power of TCS. TCS was laboratory prepared in a novel paste formula, unlike the slurry formula incorporated in previous studies. The tested null hypothesis was that there was no significant difference among the prepared TCS, CPP-ACP, and SDF-potassium iodide (SDF-KI) in the remineralization of subsurface enamel lesions at 50, 100, and 150 μm .

Methods

Materials used in the study according to the manufacturer's recommendations are listed in Table 1.

Thirty permanent caries-free human molars were collected for the study. The molars were collected from Oral and Maxillofacial Surgery Department in Faculty of Dentistry, Mansoura University. The protocol of teeth collection and storage was approved by the Mansoura University Faculty of Dentistry ethical committee (approval no. M03060819). Patients who voluntarily donated their "waste" extracted teeth provided informed consent to collect the teeth for the experimental study. The collected teeth were rinsed with deionized water and cleaned with periodontal curesttes to remove any soft-tissue debris. The teeth were stored in 0.1% thymol solution and refrigerated at 4 °C until use. The teeth were checked visually using an LED light and magnifying loupes $\times 3.5$ (Amtech, America) to detect the presence of any enamel surface defects or microcracks. Teeth with buccal surface cracks or stains were excluded from the study.

Thirty molars were subjected to the demineralization protocol, which will be discussed in detail in the following section. The demineralized specimens were divided into three groups ($n = 10$) according to the applied remineralizing agent. The demineralized specimens were treated with SDF-KI (Riva Star; Group A), CPP-ACP cream (GC Tooth Mousse; Group B), and prepared TCS paste (Group C).

Preparation of artificial carious lesions. To create enamel surface lesions resembling naturally developed WSLs, the buccal surface of the teeth was polished with 600, 800, and 1200 grit paper (Fuji Star, Sankyo Rikagaku, Saitama, Japan) consecutively under running water to remove a prismatic enamel layer. The buccal surface was covered with adhesive tape (4×4 mm in size), and acid-resistant nail varnish was used to cover the whole surface of each tooth. The tape was removed, leaving a 4×4 mm window on the buccal surface. The extracted teeth were immersed in a demineralizing solution (demineralizing solution composed of 2.2 mM calcium chloride, 2.2 mM sodium phosphate, and 0.05 M acetic acid with 1 M potassium hydroxide to obtain a pH of 4.4) for 72 h at 37 °C¹⁷. The demineralizing solution was changed every 24 h to keep the pH constant. The 30 demineralized molars were cut carefully at the level of the cemento-enamel junction to keep the crowns only using a low-speed diamond saw (Isomet; Buehler, Lake Bluff, IL, USA). The crowns were fixed in acrylic blocks then sectioned vertically under running water in the buccolingual direction using a low-speed diamond saw (Isomet; Buehler). Two halves were present. One was used as a self-control specimen, and the other was used as an experimental one.

After obtaining 60 halves of the demineralized specimens, the internal surface of the specimens that would be subjected to a cross-sectional microhardness (CSMH) test was abraded using silicon carbide paper and lapped with a cloth. The silicon carbide paper was attached to a rotary electric polishing machine (Ecomet 250; Buehler).

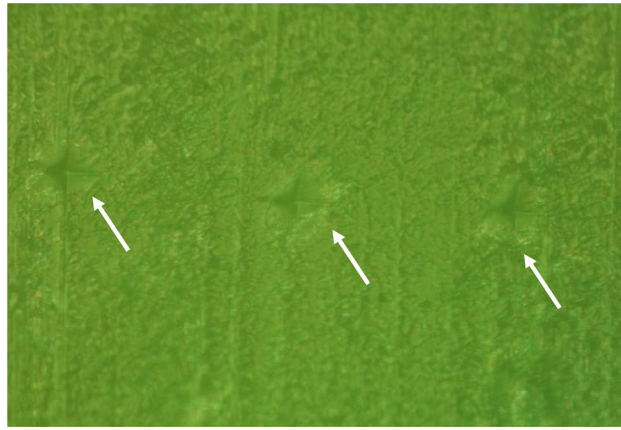


Figure 1. Microscopic image from a microhardness optical microscope ($\times 40$) showing the power of microindentations at three different points (50, 100, and 150 μm) from the external enamel surface (white arrows).

The used silicon carbide polishing papers were changed after every five specimens¹⁸. The 30 halves of the self-control specimens were fixed in acrylic blocks with their buccal or lingual surface embedded in acrylic blocks and their internal surface facing upward. The self-control halves were kept in deionized water until they were tested. The other 30 experimental halves were subjected to the treatment protocol that will be discussed thereafter.

Preparation of the TCS paste. The optimized gel was prepared according to the following protocol. First, the gelatin solution was prepared by dissolving 2.5% (w/v) gelatin in hot distilled water, and a magnetic stirrer was employed at 200 rpm and 70 °C for 30 min until complete dissolution (hot plate and magnetic stirrer; Misung Scientific Co., Korea). Simultaneously, a 2.5% (w/v) CMC solution was prepared by heating its aqueous solution to 60 °C to 70 °C in distilled water with stirring at 200 rpm using a magnetic stirrer. Sequential polymerization was induced through electrostatic interaction by adding CMC solution to the gelatin solution dropwise under magnetic stirring for 15 min at 70 °C and 200 rpm to obtain a homogenized hydrogel¹⁹. The solution was left overnight at room temperature to ensure complete mixing and gel formation. A 5 g TCS powder with a particle size of 1 to 10 μm was levigated with propylene glycol (2 mL). The levigated 5% (w/v; maximum dose) TCS was added slowly and mixed to this hydrogel using a homogenizer (Heidolph, Germany). Methylparaben (0.1%, w/v) was used as a preservative. A few drops of 1 N HCl were added to adjust the pH to the desired level (pH 6.8) and maintain the viscosity of the paste. The remaining amount of water was added with gentle stirring at room temperature to prevent the formation of air bubbles until paste formation. The pH of the paste was monitored using a pH probe (Denver Instrument Ub-10 Bio Kit, 115 VAC, USA). Finally, the prepared paste was filled in a collapsible aluminum tube until use.

Surface treatment methods. The internal surface (cross-section) of the experimental halves was covered with an adhesive tape to ensure that the treatment was subjected only to the external enamel surface. The experimental halves in Group A were painted buccally through the window by a micro brush with SDF-KI according to the manufacturer's instructions (only one time as a professional application). Specimens in Group B were painted buccally through the window by a micro brush with CPP-ACP according to the manufacturer's instructions (twice daily). The cream was left on the superficial buccal surface for 3 min, and the specimens were washed with deionized water for 5 s. Specimens in Group C were painted buccally through the window by a micro brush with the prepared TCS paste (twice daily). The paste was left on the superficial buccal surface for 3 min, and the specimens were washed with deionized water for 5 s. The experimental halves were stored in artificial saliva during the remineralization period (30 days) and kept in an incubator at 37 °C. The composition of artificial saliva was as follows: methyl-p-hydroxybenzoate (2 g/L), sodium CMC (10 g/L), $\text{CaCl}_2 \cdot 2\text{H}_2\text{O}$ (0.166 g/L), KH_2PO_4 (0.3 g/L), K_2HPO_4 (0.8 g/L), and KCl (0.6 g/L) adjusted to pH 6.8²⁰. Artificial saliva was replaced with fresh artificial saliva every 24 h to maintain the pH constant²¹. After completion of the remineralization period, the experimental halves were subjected to the same tests as the self-control halves.

CSMH test for self-control specimens. Vickers CSMH test was applied with a force of 100 g for 10 s (Wilson® Tukon 1102/1202 Series; Buehler) at three different points (50, 100, and 150 μm ; at the middle third) from the external enamel surface. These three indentations were determined and measured from the external enamel surface via the microhardness microscope annotation tool (Fig. 1).

Micro-Raman spectroscopy analysis. A specimen from each treatment group was subjected to micro-Raman spectroscopy (RAMANtouch; Nanophoton Co., Ltd., Osaka, Japan) to detect the mineral composition at the same three beforementioned points. The excitation light used was a green laser beam with a wavelength of 532 nm in the spectral range of 400 to 1200 cm^{-1} . Micro-Raman spectra were obtained using a $\times 50$ objec-

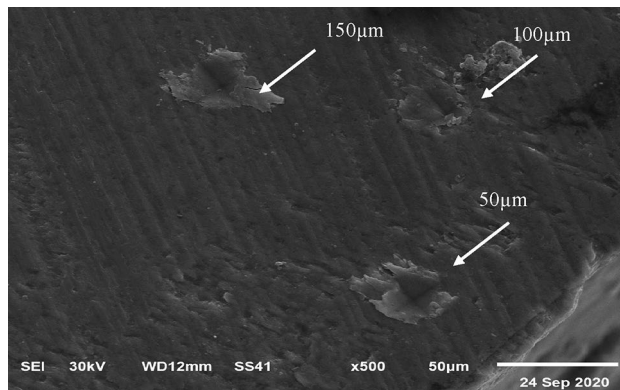


Figure 2. SEM micrograph showing microhardness indentations at 50, 100, and 150 μm (white arrows) from the external enamel surface. Micro-Raman spectroscopy and EDX were performed at the same points.

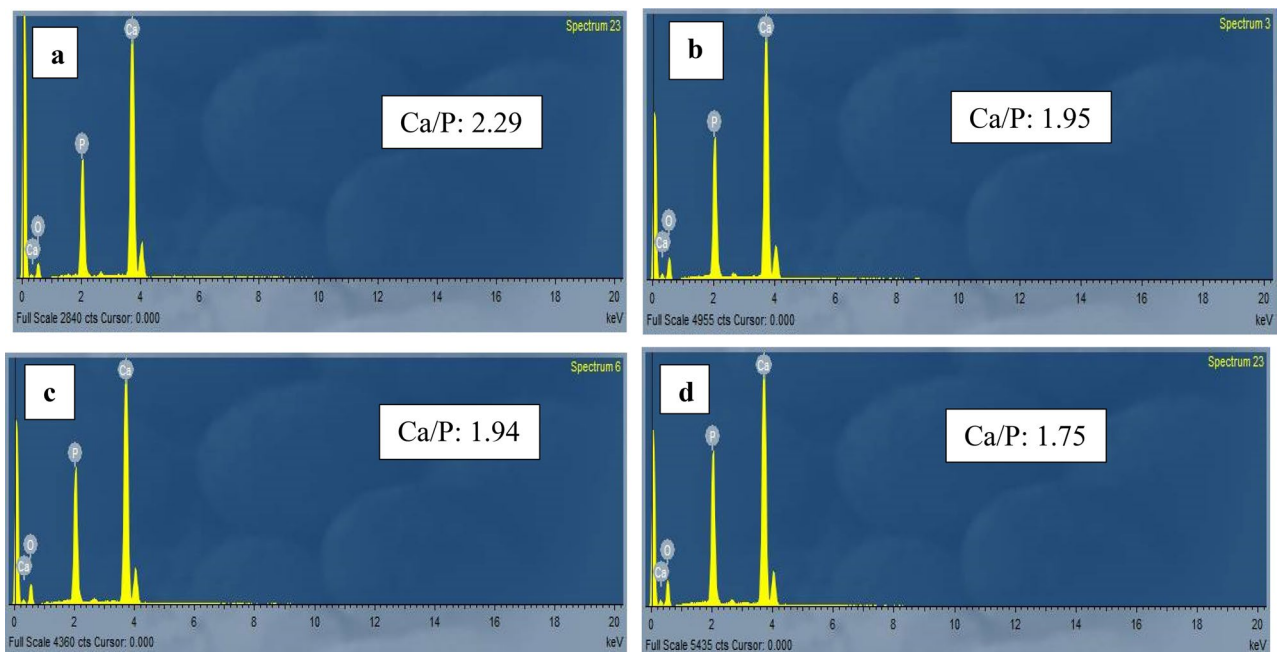


Figure 3. EDX of the remineralized specimen showing the Ca/P ratio at 150 μm : (a) prepared TCS, (b) CPP-ACP, (c) SDF-KI, and (d) control specimen.

tive to focus the laser beam on previously defined indentation points (Fig. 2). Origin version 6.1 (OriginLap, Northampton, MA, USA) and Peakfit version 4.0 (Aspire Software International, Ashburn, VA, USA) were used to analyze Raman spectra. The ratio of ν_1 PO_4^{3-} (960 cm^{-1}), ν_2 PO_4^{3-} (431 cm^{-1}), and ν_4 PO_4^{3-} (589 cm^{-1}) and B-type carbonate ν_1 CO_3^{2-} (1072 cm^{-1}) was obtained, but ν_1 PO_4^{3-} (960 cm^{-1}) and B-type carbonate ν_1 CO_3^{2-} (1072 cm^{-1}) were generalized to analyze the change in mineral composition among the specimens.

Elemental analysis using energy-dispersive X-ray spectroscopy (EDX). The specimens were removed from acrylic blocks and coated with gold sputter to be evaluated with high vacuum field emission microscopy. The images were obtained using a secondary electron detector (Everhart–Thornley) at a distance of 10 mm with a high voltage of 30 kV and magnification ranging from $\times 500$ to $\times 10,000$. The EDS spectrometer was coupled with a scanning electron microscope (SEM; JEOL Ltd., USA) to quantitatively analyze the enamel mineral content. The EDX detector represented the calcium and phosphate weight percentages in a histogram plot (Fig. 3). The specimens were subjected to elemental analysis by EDX at the same three points (Fig. 2). Finally, micromorphological scanning with SEM at the superficial buccal surface (window site) was done.

Statistical analysis. A sample size calculation with an estimated effect size of 0.60, an α of 5%, and a power of 85% resulted in a total sample size of 30 ($n = 10$ per group). The SPSS program (IBM SPSS Statistics, IBM, Armonk, NY, USA) was used to calculate descriptive statistics. Statistical analysis of the data was done, testing

Material	Specimens	n	Microhardness (mean \pm SD)		
			50 μ m	100 μ m	150 μ m
SDF-KI	Demineralized	10	216.60 \pm 46.22	244.90 \pm 52.24 ^A	261.40 \pm 48.62 ^A
	Remineralized	10	260.70 \pm 21.87 ^{ab}	288.20 \pm 19.79 ^{bc}	299 \pm 19.86 ^{bc}
CPP-ACP	Demineralized	10	190 \pm 51.66	216.30 \pm 55.87 ^A	226.90 \pm 50.55
	Remineralized	10	255.60 \pm 45.11 ^a	283.40 \pm 45.19	297.7 \pm 40.40 ^a
TCS	Demineralized	10	173.60 \pm 59.20	191.20 \pm 63.67	209.2 \pm 63.07 ^A
	Remineralized	10	268.80 \pm 29.23 ^a	293.10 \pm 29.23	307.60 \pm 30.68 ^a

Table 2. Mean \pm SD of CSMH of the different groups at different levels. ^{ABC}Similar superscript capital letters in the same column denote a significant difference among different materials within the same level on the same side (demineralized/remineralized; $p < 0.05$). ^{abc}Similar superscript lowercase letters in the same row denote a significant difference among different levels within the same material on the same side (demineralized/remineralized; $p < 0.05$). [§]Non-significant difference between the demineralized and remineralized specimens for the same level in the same material.

the normality using the Kolmogorov–Smirnov test applied before conducting the parametric tests [analysis of variance (ANOVA) and Tukey's post hoc test]. Statistical significance was predetermined at $p < 0.05$.

Ethical approval. The local Institutional Ethical Committee granted ethical approval for the current study under approval number (M03060819). All procedures performed in the study were in accordance with 1964 Helsinki Declaration and its later amendments or comparable ethical standards.

Clinical relevance. The tricalcium silicate paste used in this study is a promising remineralizing agent for treating incipient lesions.

Results

CSMH results. In the three-way ANOVA, there was no significant difference in the remineralization potential among the different groups ($p > 0.05$). The mean \pm standard deviation (SD) of the demineralized and remineralized specimens in the three different groups at three different levels (50, 100, and 150 μ m) are shown in Table 2.

The mean \pm SD and Tukey's post hoc test multiple comparisons revealed a significant difference between the demineralized and remineralized specimens in the three different groups at the three different levels (50, 100, and 150 μ m; $p < 0.05$). This reflected the remineralization power of the three tested materials. There was no significant difference among the specimens remineralized with SDF-KI, CPP-ACP, and TCS at the three different levels. There was a significant difference among the enamel microhardness at 50 and 150 μ m in the three remineralized groups, reflecting the penetration power of the three tested materials.

There was a significant difference between demineralized specimens in the CPP-ACP and SDF-KI groups at 100 μ m and the TCS and SDF-KI groups at 150 μ m. Such discrepancies among demineralized specimens can be attributed to the following—the examined sound molars were collected from different patients of different ages. Age changes in old patients may compromise the hardness and mineral content of the sound enamel. Also, some of the examined molars were impacted molars, meaning that they had limited exposure to intraoral acidic cycles.

EDX results. In the three-way ANOVA, there was a significant difference in Ca/P ratio among the different groups ($p < 0.05$). The mean \pm standard deviation (SD) of the demineralized and remineralized specimens in the three different groups at three different levels (50, 100, and 150 μ m) are shown in Table 3.

The mean \pm SD and Tukey's post hoc test revealed a significant difference in the Ca/P ratio between the demineralized and remineralized specimens in the TCS group at the three different levels ($p < 0.05$).

Regarding CPP-ACP and SDF-KI, the significant difference in the Ca/P ratio between the demineralized and remineralized specimens was recorded at 50 and 100 μ m ($p < 0.05$). At 150 μ m, there was no significant difference between the demineralized and remineralized specimens ($p > 0.05$).

Also, there was a significant difference among the remineralized specimens in the three groups at 50 μ m ($p < 0.05$). There was also a significant difference between the specimens remineralized with SDF-KI and TCS at 100 and 150 μ m ($p < 0.05$). Prepared TCS showed the highest Ca/P ratio.

The major bands or parameters that can describe the mineral composition through micro-Raman spectroscopy corresponded to the phosphate (PO_4^{3-}) and carbonate (CO_3^{2-}) groups. The phosphate group was associated with HAp crystals and had different vibration frequencies. The major vibration frequency of $\nu_1 \text{PO}_4^{3-}$ was near 960 cm^{-1} , whereas other minor vibration frequencies of ν_2 and $\nu_4 \text{PO}_4^{3-}$ vibrations were detected near 431 and 589 cm^{-1} , respectively. The vibration of $\nu_1 \text{CO}_3^{2-}$ (B-type substitute) was detected near 1072 cm^{-1} ²². The intensity of bands assigned to CO_3^{2-} reflected the carbonate content in the enamel and their substitution, which may be A- or B-type substitution. When the OH^- group is substituted by the CO_3^{2-} group, this is defined as an A-type substitution, whereas a B-type substitution is expressed when the PO_4^{3-} group is substituted by a CO_3^{2-} one. The carbonate content revealed sufficient information about enamel hardness²². The increase in the intensity of the $\nu_1 \text{CO}_3^{2-}$ band is an indicator of reduction in enamel hardness and its higher susceptibility to dissolution during

Treatment material	Specimens	n	Ca/P ratio (mean \pm SD)		
			50 μ m	100 μ m	150 μ m
SDF-KI	Demineralized	10	1.69 \pm 0.21	1.78 \pm 0.21	1.84 \pm 0.37 ⁵
	Remineralized	10	1.97 \pm 0.12 ^A	1.95 \pm 0.07 ^A	1.92 \pm 0.12 ^B
CPP-ACP	Demineralized	10	1.63 \pm 0.18	1.73 \pm 0.20	1.79 \pm 0.34 ⁵
	Remineralized	10	1.96 \pm 0.13 ^B	2.00 \pm 0.11	1.99 \pm 0.14
TCS	Demineralized	10	1.63 \pm 0.12	1.66 \pm 0.102	1.67 \pm 0.14
	Remineralized	10	2.09 \pm 0.13 ^{AB}	2.09 \pm 0.155 ^A	2.09 \pm 0.16 ^B

Table 3. Mean \pm SD of Ca/P ratio of different groups at different levels. ^{ABC} Similar superscript capital letters in the same column denote a significant difference among different materials within the same level on the same side (demineralized/remineralized). ^{abc} Similar superscript lowercase letters in the same row denote a significant difference among different levels within the same material on the same side (demineralized/remineralized). ⁵ Nonsignificant difference between demineralized and remineralized sides for the same concentration in the same material.

acidogenic attacks. The high intensity of the ν_1 PO_4^{3-} band indicated a high level of enamel mineralization²². All spectra were normalized based on the major vibration frequency ν_1 PO_4^{3-} , as it showed the most intense peak (Fig. 4). Specimens treated with TCS showed the highest intensity of ν_1 PO_4^{3-} at the three different levels, whereas specimens treated with SDF-KI showed the lowest band intensity. SDF-KI also showed the highest intensity of the ν_1 CO_3^{2-} band at 50 μ m, reflecting the lowest remineralization power compared to CPP-ACP and TCS.

Micromorphological analysis. SEM of demineralized (self-control) specimens at high magnification ($\times 2000$) showed observable pitting, discontinuity, and surface irregularity resulting from the destruction of enamel rods and the dissolution of enamel crystals during the demineralization process (Fig. 5a).

In the enamel substrate treated with CPP-ACP, SEM indicated the ability of CPP-ACP to restore the uniform, thick, and compact layer of disaggregated nanoclusters with a globular structure that decreased the size of interprismatic cavities (Fig. 5b).

SEM of enamel substrate treated with SDF-KI showed the ability of the SDF-KI solution to infiltrate the demineralized enamel, forming dense non-uniform crystals that well-sealed enamel interprismatic cavities (Fig. 5c).

SEM of the enamel substrate treated with experimental TCS indicated the ability of TCS paste to restore the uniform, compact, and homogenous layer of calcific deposits that well-sealed interprismatic cavities. The enamel substrate appeared with a low level of superficial roughness (Fig. 5d).

Discussion

The null hypothesis of this study was partially accepted. The microhardness test revealed no significant difference in the remineralization potential of the three different materials at the three different levels (50, 100, and 150 μ m). The EDX test revealed a significant difference among the three different materials at three levels.

The microhardness test is one of the most widely used tests to measure the mechanical properties and structural integrity of materials or substrates. Such an easy, simple, and nondestructive approach requires a limited specimen area to be tested. The specimen surface is impressed with a square-diamond indentation at a certain load for a certain period. After removing the load, the diagonal imprint is measured using an optical microscope to determine the length of the diagonal and size of the imprint²³.

EDX is a quantitative X-ray microanalytical technique that provides sufficient information about the chemical composition of the targeted area of a sample. Such technology is based on the emission of a characteristic X-ray through a filament toward the sample²⁴. An EDX detector can represent specific elements in a histogram plot with the number of counts against the X-ray energy²⁴. Also, this powerful equipment combined with SEM magnifies and scans the area of interest and detects micromorphological changes²⁵.

Schlueter et al.²⁶ categorized SEM-EDX as a semiquantitative approach for elemental analysis. Cochrane et al.²⁷ considered that the utilization of electron probe microanalysis generating X-ray in quantifying enamel mineral changes is a highly problematic approach. They addressed a list of drawbacks related to such technology, including non-uniform porosity that may cause density variations, an observed reduction of generated X-ray, and low interaction volumes for nonhomogeneous samples²⁷. All these drawbacks justify using SEM-EDX in conjunction with another quantitative approach. The outcomes of this study are in line with Schlueter et al.'s²⁶ and Cochrane et al.'s²⁷ assumptions, as CSMH and SEM-EDX results did not totally confirm each other. Therefore, one specimen from each treatment group was subjected to micro-Raman spectroscopy. Raman spectroscopy is a quantitative, analytical, nondestructive approach that can detect the molecular level and composition by irradiating the specimen with a visible laser source²⁸. Micro-Raman spectroscopy revealed that the most intensive ν_1 PO_4^{3-} band was detected in the remineralized specimen with TCS at three levels (50, 100, and 150 μ m). Specimens treated with CPP-ACP and SDF-KI showed the weak intensity of the ν_1 PO_4^{3-} band.

Recently, the professional application of SDF-KI has gained wide acceptance due to its safety and effectiveness in either arresting or remineralizing early enamel surface lesions. Although sodium fluoride varnish is considered the gold standard protocol for enamel remineralization, SDF has shown comparable remineralization potential²⁹. An in vitro study revealed the role of KI application to SDF in reducing the black staining effect

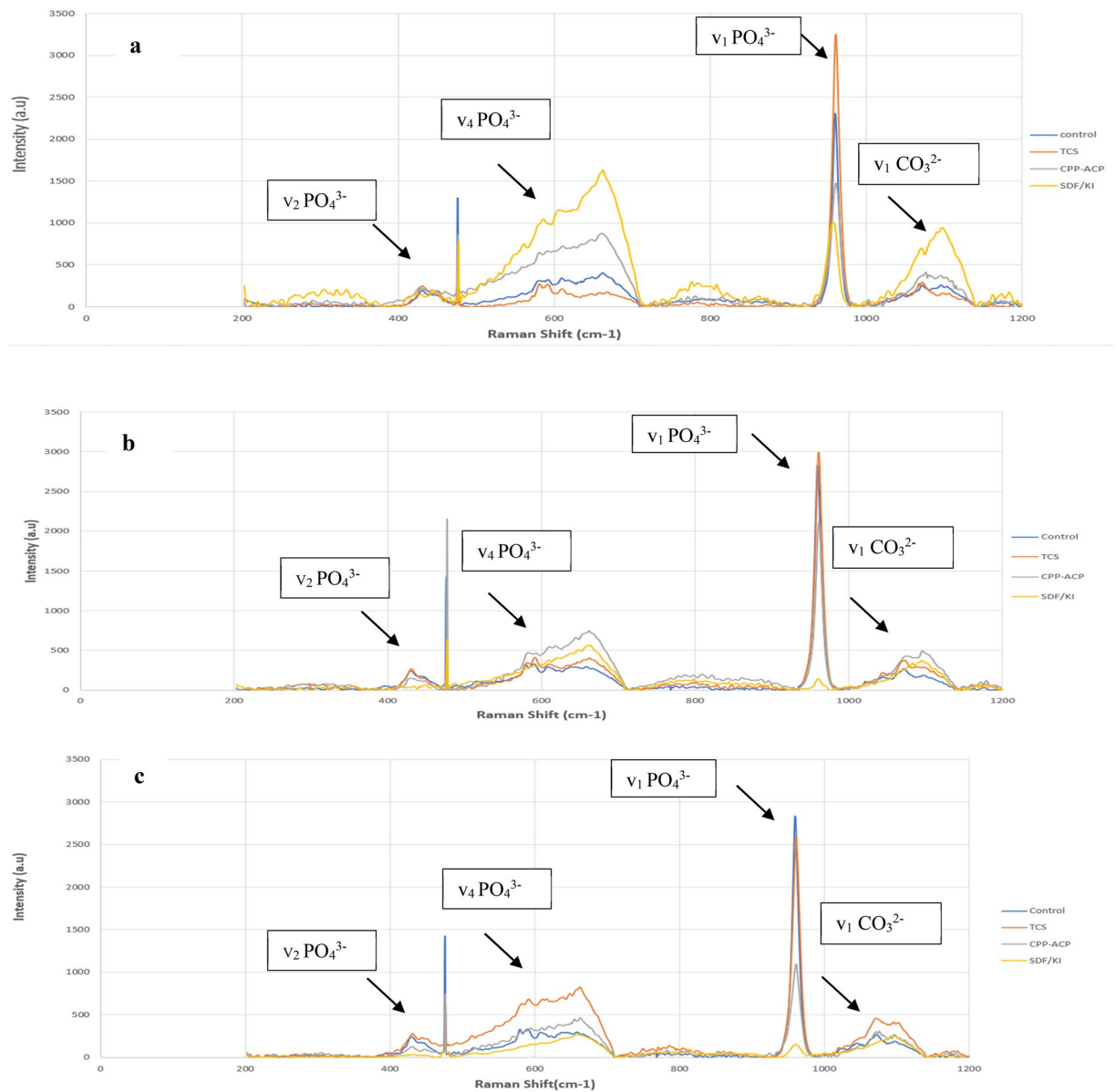


Figure 4. Micro-Raman spectroscopy of remineralized specimens showing the intensity of phosphate ($v_1 \text{PO}_4^{3-}$) and carbonate ($v_1 \text{CO}_3^{2-}$) bands at three different levels: (a) 50 μm , (b) 100 μm , and (c) 150 μm .

and increasing enamel microhardness. SDF-KI showed potential rehardening of demineralized enamel than SDF alone³⁰. According to published evidence SDF-KI was incorporated in the current study as a representative of fluoride-based remineralizing products. Punhagui et al.⁹ concluded that the application of 38% SDF or even 30% SDF has a significant remineralization effect on the enamel surface and CSMH. Punhagui et al.⁹ conducted the enamel CSMH test at 10, 20, 50, 70, and 90 μm on deciduous enamel. However, the study is in line with Punhagui et al., citing that Punhagui et al.'s study may be considered weak evidence. Deciduous teeth have different pore sizes and mineral content than permanent teeth³¹. Also, this study is in total agreement with Barrera Ortega et al.'s³² study, which was conducted on permanent molars like this one. Barrera Ortega et al.³² evaluated the remineralization power of SDF by performing the CSMH test. They assumed that SDF increased the enamel microhardness up to 150 μm , in line with this study. The remineralization power of SDF was brilliantly explained by Mei et al.³³. Mei et al.³³ demonstrated that SDF could react with a salivary component, such as calcium and phosphate ions, forming fluorapatite crystals. These crystals can act as a nucleation site for further fluorapatite precipitates. Also, such crystals can promote ion exchange of F^- for OH^- . Mei et al.³³ also revealed an increase in the vibration frequency of phosphate peaks using Raman spectra, reflecting OH^- substitution with further F^- ions.

CPP-ACP has shown a satisfactory remineralization effect in different studies, and such an effect has been discussed previously in several cariology studies^{34,35}. CPP contains Ser(P)-Ser(P)-Ser(P)-Glu-Glu sequence that can stabilize calcium, phosphate, and hydroxide ions as an amorphous nanocomplex (ACP), preventing rapid phase transformation³⁵. Likewise, CPP-ACP can be localized on tooth surface buffering free calcium and phosphate

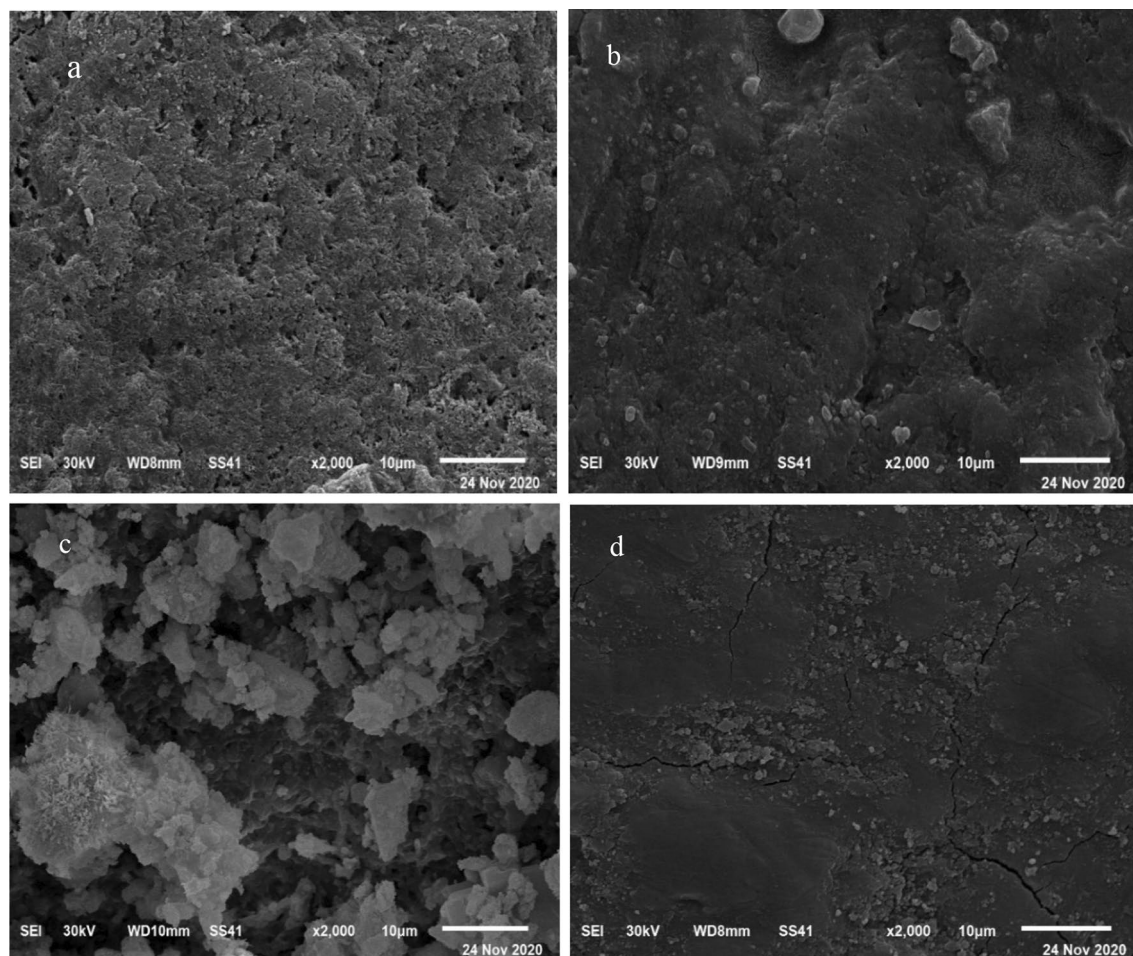


Figure 5. (a) SEM micrograph of a demineralized enamel surface. (b) SEM micrograph of an enamel substrate treated with CPP-ACP. (c) SEM of an enamel substrate treated with SDF-KI. (d) SEM micrograph of an enamel substrate treated with prepared TCS.

ions, maintaining a state of supersaturation³⁵. This study evaluated the remineralization potential of CPP-ACP on enamel subsurface lesions. This study agrees with previous similar studies^{13,36}. Oliveira et al.¹³ concluded that MI paste could significantly reduce the demineralization effect on the outer enamel surface. Their CSMH indentations were conducted at 25, 50, 75, 100, 125, 150, 175, 200, 225, and 250 μm from the external enamel surface. They assumed that the MI paste showed a rehardening effect on the enamel subsurface up to 75 μm . This seems to be in partial agreement with this study. The slight difference in the findings between both may be ascribed to the length of each experiment. The length of Oliveira et al.'s study was 10 days, whereas the length of this study was 30 days. Also, CPP-ACP was applied once daily in Oliveira et al.'s study, whereas it was applied twice daily in this study, justifying the slight difference between the findings. Another in vitro study showed the opposite results to this study³⁷. The in vitro study demonstrated that CPP-ACP failed to remineralize the artificially created enamel subsurface lesion at 150 μm ³⁷. Such contradiction in results was attributable to the difference in the length and design of each study. The remineralization protocol of the in vitro study was based on applying a remineralizing agent, followed by pH cycling for 5 consecutive days only. Overall, the study was in accordance with Reynolds et al.'s assumption about the remineralization of subsurface enamel lesions using CPP-ACP³⁸. Reynolds et al.³⁸ highlighted the ability of the CPP-ACP nanocomplex to tightly bind to the enamel substrate, providing a reservoir of bioavailable calcium and phosphate ions. Microradiographs also recorded the ability of such bioavailable minerals to remineralize the body of the lesion³⁸. The EDX revealed a higher Ca/P ratio of remineralized tissue than in normal HAp, in accordance with this study³⁸.

Calcium silicate-based materials have an expanded range in restorative dentistry. One of the biggest advantages of these materials is their bioactivity, meaning that the material can react with body fluids producing mineral infiltration and deposition. Regarding enamel remineralization, there is little evidence suggesting using calcium silicate-based material in enamel remineralization¹⁵. An in vitro study demonstrated that when TCS (Ca_3SiO_4) comes in contact with saliva, it dissolves, forming a silanol group (si-o) that induces the precipitation of HAp¹⁵. Such a silanol group is characterized by obtaining triple junctions per unit area, which can provide a stereochemical match for oxygen atoms that will bond to Ca^{2+} ions¹⁵. Negatively charged PO_4^{3-} ions in human saliva can be electrostatically attracted to positively charged Ca^{2+} ions, forming a dense Ca-P mineralized layer.

An in vitro study also demonstrated the remineralization power of TCS in a slurry formula on the demineralized enamel¹⁶.

Parker et al.³⁹ evaluated the repairable and protective effects of calcium silicate on sound and eroded enamel. Parker et al. assumed that micro-Raman spectra obtained from calcium silicate showed characteristic peaks similar to HAp³⁹. Other in vitro and in situ experiments identified HAp formation on the enamel surface after brushing with a slurry of calcium silicate⁴⁰. In vitro studies that evaluated the remineralization potential of TCS used it in the slurry formula. The clinical application of TCS in slurry form may be very difficult for patients. Furthermore, TCS formulation in such a manner may be time- and material-consuming each time. Therefore, in this study, TCS was prepared in a paste form for easy application in future clinical research if it showed promising results. Also, TCS in a paste formula can be tightly bound to the enamel substrate, providing biofilm supersaturation with minerals, maximizing its remineralization potential. Such formula was inspired by similar bioactive remineralizing products with the same remineralization rationale, such as Novamin paste and 45S5 Bioactive glass^{41–43}. Generally speaking, regarding the remineralization power of TCS, the discussed evidence in the literature agrees with this study. Although several biological components, such as proteins and extracellular matrix, are involved in enamel mineralization and crystal nucleation, TCS showed potential remineralization that may compel community research to investigate further. In this study, specimens treated with TCS showed promising rehardening of the softened enamel up to 150 µm. Also, EDX results showed a superior remineralization power of TCS on subsurface enamel lesions up to 150 µm compared to CPP-ACP and SDF-KI. Micro-Raman spectroscopy also supported EDX findings, as the highest ν_1 PO_4^{3-} band intensity was observed in the specimen treated with TCS at three levels. Therefore, TCS is superior in remineralization and penetration ability in artificial enamel lesions.

Human saliva plays a crucial role in enamel remineralization, as it contains organic components (e.g., glycoproteins) and inorganic components (e.g., calcium, phosphate, and fluoride). When the human saliva gets out of the oral environment, its protective effect may be compromised due to changes in its composition²⁰. Collecting human saliva is also very difficult and time-consuming. Due to the limitations of using natural saliva in in vitro studies, substitutive formulations must be available to simulate the oral environment in remineralization studies²⁰. Different formulations of artificial saliva are available for remineralization studies. There is no consensus in cariology research on the ideal formula to be used in remineralization studies²⁰. The used formula in this study had shown the lowest remineralization power compared to four different formulas²⁰. The formula of the used artificial saliva in this study contains carboxymethyl cellulose. CMC increases the viscosity of the artificial saliva solution, consequently limiting the mineral diffusion to the enamel substrate²⁰. Also, CMC can form complexes between calcium and phosphate ions, resulting in the unavailability of such minerals in enamel remineralization²⁰. The rationale behind selecting such a formula is to provide some sort of accurate evaluation of tested materials and avoid generating misleading results.

The outcomes of the current study are limited by comparing tricalcium silicate paste with single material (CPP-ACP) that belongs to the same category (bioavailable calcium phosphate remineralizing system). It would be better if another bioactive material were included in the study. This will be considered in the future studies.

Conclusion

In this study, prepared TCS paste was a powerful remineralizing agent for managing early enamel lesions. Prepared TCS showed that the remineralization power of enamel subsurface lesions reached up to 150 µm. This approach seems to be a safe and effective remineralization approach for managing early enamel carious lesions.

Data availability

The data that support the findings of the current study are available from corresponding author upon reasonable request.

Received: 23 March 2022; Accepted: 17 May 2022

Published online: 15 June 2022

References

- Ismail, A. I. et al. The International Caries Detection and Assessment System (ICDAS): An integrated system for measuring dental caries. *Commun. Dent. Oral Epidemiol.* **35**, 170–178. <https://doi.org/10.1111/j.1600-0528.2007.00347.x> (2007).
- Alaffi, A., Yassen, A. A. & Hassanein, O. E. Effectiveness of polyacrylic acid-bioactive glass air abrasion preconditioning with NovaMin remineralization on the microhardness of incipient enamel-like lesion. *JCD* **22**, 548–553. https://doi.org/10.4103/jcd.jcd_195_19 (2019).
- Balakrishnan, A., Jonathan, R., Benin, P. & Kuumar, A. Evaluation to determine the caries remineralization potential of three dentifrices: An in vitro study. *JCD* **16**, 375–379. <https://doi.org/10.4103/0972-0707.114347> (2013).
- Rošin-Grget, K., Peroš, K., Sutej, I. & Bašić, K. The cariostatic mechanisms of fluoride. *Acta Med. Acad.* **42**, 179–188. <https://doi.org/10.5644/ama2006-124.85> (2013).
- Tulumbaci, F. & Oba, A. A. Efficacy of different remineralization agents on treating incipient enamel lesions of primary and permanent teeth. *JCD* **22**, 281–286. https://doi.org/10.4103/jcd.jcd_509_18 (2019).
- Contreras, V., Toro, M. J., Elias-Boneta, A. R. & Encarnación-Burgos, A. Effectiveness of silver diamine fluoride in caries prevention and arrest: A systematic literature review. *Gen. Dent.* **65**, 22–29 (2017).
- Trieu, A., Mohamed, A. & Lynch, E. Silver diamine fluoride versus sodium fluoride for arresting dentine caries in children: A systematic review and meta-analysis. *Sci. Rep.* **9**, 2115. <https://doi.org/10.1038/s41598-019-38569-9> (2019).
- Rosenblatt, A., Stamford, T. C. & Niederman, R. Silver diamine fluoride: A caries “silver-fluoride bullet”. *J. Dent. Res.* **88**, 116–125. <https://doi.org/10.1177/0022034508329406> (2009).
- Punhagui, M. F. et al. Effect of application time and concentration of silver diamine fluoride on the enamel remineralization. *J Clin Exp Dent* **13**, e653–e658. <https://doi.org/10.4317/jced.58318> (2021).

10. Punyanirun, K., Yospiboonwong, T., Kunapinun, T., Thanyasrisung, P. & Trairatvorakul, C. Silver diamine fluoride remineralized artificial incipient caries in permanent teeth after bacterial pH-cycling in-vitro. *J. Dent.* **69**, 55–59. <https://doi.org/10.1016/j.jdent.2017.09.005> (2018).
11. Jefferies, S. R. Advances in remineralization for early carious lesions: A comprehensive review. *Compendium of Continuing Education In Dentistry (Jamesburg, NJ: 1995)* **35**, 237–243 (2014).
12. Thierens, L. A. M. et al. The in vitro remineralizing effect of CPP-ACP and CPP-ACPF after 6 and 12 weeks on initial caries lesion. *J. Appl. Oral Sci. Rev. FOB* **27**, e20180589. <https://doi.org/10.1590/1678-7757-2018-0589> (2019).
13. Oliveira, P. R. A., Barboza, C. M., Barreto, L. & Tostes, M. A. Effect of CPP-ACP on remineralization of artificial caries-like lesion: An in situ study. *Braz. Oral Res.* **34**, e061. <https://doi.org/10.1590/1807-3107bor-2020.vol34.0061> (2020).
14. Cross, K. J., Huq, N. L. & Reynolds, E. C. Casein phosphopeptide-amorphous calcium phosphate nanocomplexes: A structural model. *Biochemistry* **55**, 4316–4325. <https://doi.org/10.1021/acs.biochem.6b00522> (2016).
15. Dong, Z., Chang, J., Joiner, A. & Sun, Y. J. D. S. Tricalcium silicate induces enamel remineralization in human saliva. *J. Dental Sci.* **8**, 440–443 (2013).
16. Wang, Y., Li, X., Chang, J., Wu, C. & Deng, Y. Effect of tricalcium silicate (Ca₃SiO₅) bioactive material on reducing enamel demineralization: an in vitro pH-cycling study. *J. Dent.* **40**, 1119–1126. <https://doi.org/10.1016/j.jdent.2012.09.006> (2012).
17. Oliveira, P., Fonseca, A., Silva, E. M., Coutinho, T. & Tostes, M. A. Remineralizing potential of CPP-ACP creams with and without fluoride in artificial enamel lesions. *Aust. Dent. J.* **61**, 45–52. <https://doi.org/10.1111/adj.12305> (2016).
18. Ishak, H., Field, J. & German, M. Baseline specimens of erosion and abrasion studies. *Eur. J. Dent.* **15**, 369–378. <https://doi.org/10.1055/s-0040-1721235> (2021).
19. Sathish, P. B. et al. Tricomposite gelatin-carboxymethylcellulose-alginate bioink for direct and indirect 3D printing of human knee meniscal scaffold. *Int. J. Biol. Macromol.* **195**, 179–189. <https://doi.org/10.1016/j.ijbiomac.2021.11.184> (2022).
20. Ionta, F. Q. et al. In vitro assessment of artificial saliva formulations on initial enamel erosion remineralization. *J. Dent.* **42**, 175–179. <https://doi.org/10.1016/j.jdent.2013.11.009> (2014).
21. Kim, H. N., Kim, J. B. & Jeong, S. H. Remineralization effects when using different methods to apply fluoride varnish in vitro. *J. Dental Sci.* **13**, 360–366. <https://doi.org/10.1016/j.jds.2018.07.004> (2018).
22. Zavala-Alonso, V. et al. Analysis of the molecular structure of human enamel with fluorosis using micro-Raman spectroscopy. *J. Oral Sci.* **54**, 93–98. <https://doi.org/10.2334/josnusd.54.93> (2012).
23. Chuenarrom, C., Benjakul, P. & Daosodsai, P. J. M. R. Effect of indentation load and time on knoop and vickers microhardness tests for enamel and dentin. *Mat. Res.* **12**, 473–476 (2009).
24. Khan, M. S. I., Oh, S. W. & Kim, Y. J. Power of scanning electron microscopy and energy dispersive X-ray analysis in rapid microbial detection and identification at the single cell level. *Sci. Rep.* **10**, 2368. <https://doi.org/10.1038/s41598-020-59448-8> (2020).
25. Scimeca, M., Bischetti, S., Lamsira, H. K., Bonfiglio, R. & Bonanno, E. Energy Dispersive X-ray (EDX) microanalysis: A powerful tool in biomedical research and diagnosis. *EJH* **62**, 2841. <https://doi.org/10.4081/ejh.2018.2841> (2018).
26. Schlueter, N., Hara, A., Shellis, R. P. & Ganss, C. Methods for the measurement and characterization of erosion in enamel and dentine. *Caries Res.* **45**(Suppl 1), 13–23. <https://doi.org/10.1159/000326819> (2011).
27. Cochrane, N. J. et al. Comparative study of the measurement of enamel demineralization and remineralization using transverse microradiography and electron probe microanalysis. *Microsc. Microanal.* **20**, 937–945. <https://doi.org/10.1017/s1431927614000622> (2014).
28. Miyamoto, N. et al. Molecular fingerprint imaging to identify dental caries using raman spectroscopy. *Materials (Basel, Switzerland)* <https://doi.org/10.3390/ma13214900> (2020).
29. Yu, O. Y. et al. Remineralisation of enamel with silver diamine fluoride and sodium fluoride. *Dent. Mater.* **34**, e344–e352. <https://doi.org/10.1016/j.dental.2018.10.007> (2018).
30. Sorkhdini, P., Crystal, Y. O., Tang, Q. & Lippert, F. In vitro rehardening and staining effects of silver diamine fluoride with and without mucin on early enamel caries lesions. *Am. J. Dent.* **34**, 205–210 (2021).
31. Wilson, P. R. & Beynon, A. D. Mineralization differences between human deciduous and permanent enamel measured by quantitative microradiography. *Arch. Oral Biol.* **34**, 85–88. [https://doi.org/10.1016/0003-9969\(89\)90130-1](https://doi.org/10.1016/0003-9969(89)90130-1) (1989).
32. Barrera Ortega, C. C., Araiza Tellez, M. A., Garcia Perez, A. J. J. C. & Research, D. Assessment of enamel surface microhardness with different fluorinated compounds under pH cycling conditions: an in vitro study. *J. Clin. Diagn. Res.* **13**(8), 5–10 (2019).
33. Mei, M. L. et al. Formation of fluorohydroxyapatite with silver diamine fluoride. *J. Dent. Res.* **96**, 1122–1128. <https://doi.org/10.1177/0022034517709738> (2017).
34. de Oliveira, P. R. A., Barreto, L. & Tostes, M. A. Effectiveness of CPP-ACP and fluoride products in tooth remineralization. *Int. J. Dental Hygiene* <https://doi.org/10.1111/idh.12542> (2021).
35. Walker, G. D. et al. Consumption of milk with added casein phosphopeptide-amorphous calcium phosphate remineralizes enamel subsurface lesions in situ. *Aust. Dent. J.* **54**, 245–249. <https://doi.org/10.1111/j.1834-7819.2009.01127.x> (2009).
36. Cochrane, N. J., Saranathan, S., Cai, F., Cross, K. J. & Reynolds, E. C. Enamel subsurface lesion remineralisation with casein phosphopeptide stabilised solutions of calcium, phosphate and fluoride. *Caries Res.* **42**, 88–97. <https://doi.org/10.1159/000113161> (2008).
37. Lata, S., Varghese, N. O. & Varughese, J. M. Remineralization potential of fluoride and amorphous calcium phosphate-casein phospho peptide on enamel lesions: An in vitro comparative evaluation. *JCD* **13**, 42–46. <https://doi.org/10.4103/0972-0707.62634> (2010).
38. Reynolds, E. C. Calcium phosphate-based remineralization systems: Scientific evidence?. *Aust. Dent. J.* **53**, 268–273. <https://doi.org/10.1111/j.1834-7819.2008.00061.x> (2008).
39. Parker, A. S. et al. Measurement of the efficacy of calcium silicate for the protection and repair of dental enamel. *J. Dent.* **42**(Suppl 1), S21–29. [https://doi.org/10.1016/s0300-5712\(14\)50004-8](https://doi.org/10.1016/s0300-5712(14)50004-8) (2014).
40. Sun, Y. et al. Mode of action studies on the formation of enamel minerals from a novel toothpaste containing calcium silicate and sodium phosphate salts. *J. Dent.* **42**(Suppl 1), S30–38. [https://doi.org/10.1016/s0300-5712\(14\)50005-x](https://doi.org/10.1016/s0300-5712(14)50005-x) (2014).
41. Khijmatgar, S., Reddy, U., John, S., Badavannavar, A. N. & Souza, T. D. Is there evidence for Novamin application in remineralization?: A Systematic review. *J. Oral. Biol. Craniofac. Res.* **10**, 87–92. <https://doi.org/10.1016/j.jobocr.2020.01.001> (2020).
42. Abbassy, M. A., Bakry, A. S., Almoabady, E. H., Almusally, S. M. & Hassan, A. H. Characterization of a novel enamel sealer for bioactive remineralization of white spot lesions. *J. Dent.* **109**, 103663. <https://doi.org/10.1016/j.jdent.2021.103663> (2021).
43. Abbassy, M. A., Bakry, A. S., Hill, R. & Habib, H. A. Fluoride bioactive glass paste improves bond durability and remineralizes tooth structure prior to adhesive restoration. *Dental Mater.* **37**, 71–80. <https://doi.org/10.1016/j.dental.2020.10.008> (2021).

Acknowledgements

The author gratefully acknowledge Dr: Emad Abo El Azm Research Center for providing Tukon microhardness tester.

Author contributions

S.H.M, H.H.H, A.F conceived the idea of the study. K.H contributed to collection of the samples and performing cross-sectional microhardness and elemental analysis test and wrote the manuscript. A.M contributed to preparation of tricalcium silicate paste. H.H.H, K.H contributed to data acquisition, analysis and interpretation. All authors reviewed the manuscript.

Funding

Open access funding provided by The Science, Technology & Innovation Funding Authority (STDF) in cooperation with The Egyptian Knowledge Bank (EKB).

Competing interests

The authors declare no competing interests.

Additional information

Supplementary Information The online version contains supplementary material available at <https://doi.org/10.1038/s41598-022-13608-0>.

Correspondence and requests for materials should be addressed to H.H.H.

Reprints and permissions information is available at www.nature.com/reprints.

Publisher's note Springer Nature remains neutral with regard to jurisdictional claims in published maps and institutional affiliations.



Open Access This article is licensed under a Creative Commons Attribution 4.0 International License, which permits use, sharing, adaptation, distribution and reproduction in any medium or format, as long as you give appropriate credit to the original author(s) and the source, provide a link to the Creative Commons licence, and indicate if changes were made. The images or other third party material in this article are included in the article's Creative Commons licence, unless indicated otherwise in a credit line to the material. If material is not included in the article's Creative Commons licence and your intended use is not permitted by statutory regulation or exceeds the permitted use, you will need to obtain permission directly from the copyright holder. To view a copy of this licence, visit <http://creativecommons.org/licenses/by/4.0/>.

© The Author(s) 2022